Study of the End-grain Butt Joints Obtained by Friction Welding of Moso Bamboo

Haiyang Zhang,[a,*] Antonio Pizzi,[b,c] Xiaoning Lu,[a] and Zhiqiang Wang [a]

End-grain-to-end-grain welding has been the object of considerable study in the authors' laboratory, but successful experiments have been hindered by wood defibration. End-grain butt joints obtained by friction welding with moso bamboo showed relatively good experimental results compared to beech, oak, and spruce. The average compression shear strength of the welded joints reached 5.81 MPa, and the departure of the bamboo fibers could not be observed during the welding process. A study of the microstructure of the welded surface revealed that during the welding process, hard vascular bundles within the fibers became prominent on the welded surface and acted similarly to a brush. These bundles dissipated lateral friction and protected the bamboo from cracking in the process.

Keywords: Moso bamboo; Butt joints; Linear welding; Bonding strength

Contact information: a: College of Wood Science and Technology, Nanjing Forestry University, 159# Longpan Road, Nanjing 210037, China; b: LERMAB (Laboratory for the Study and Research on Wood Material), University of Lorraine, 27 rue Philippe Seguin, CS 60036, Epinal Cedex 88026, France; and c: Department of Physics, King Abdulaziz University, Jeddah, Saudi Arabia;
** Corresponding author: zhanghaiyangnjfu@gmail.com*

INTRODUCTION

Mechanically-induced linear-vibration welding, which has been used mainly in joining thermoplastics and metals, has been exploited to join wood for more than ten years (Gfeller *et al.* 2003). During this time, newer technologies have also been developed, such as rotational wood dowel welding, orbital welding, ultrasonic welding, and micro-friction stir welding (Pizzi *et al.* 2004; Tondi *et al.* 2007). These techniques for bonding block wood without additional adhesives or other chemicals are environmentally friendly and have high efficiency and energy savings. Among these wood welding techniques, linear-vibration and rotational welding have gained a great deal of research attention. The first aspect of these techniques that is being studied is the bonding of the welded joints. The microstructures of these welding interfaces and the chemical reactions that occur as the welding proceeds were used to explain the inherent mechanism behind the bonding phenomena of the welded joints (Stamm *et al.* 2005; Delmotte *et al.* 2008; Mansouri *et al.* 2010; Belleville *et al.* 2013; Zhang *et al.* 2014a; Ruponen *et al.* 2015). The second aspect of linear-vibration and rotational welding being studied is the optimization of the welding parameters for the different biomaterials and exploration of how they influence the final welding performance. Certain welding parameters, such as welding pressure, welding frequency, welding amplitude, welding time, holding pressure, and holding time are machine settings. Wood species, orientation of the wood grains, type of wood (heartwood or sapwood), number of annual rings, shape of the welded wood surface, and equilibrium moisture of the samples are all parts of the material properties that have also been studied a great deal (Properzi *et al.* 2005; Ganne-Chédeville *et al.* 2006a; Omrani *et al.* 2009;

Zhang *et al.* 2014b; Zigon *et al.* 2015; Amirou *et al.* 2016). A third aspect of both linear-vibration and rotational welding that has been studied is the creation of new, environmentally-friendly, and cost-effective products, such as "weldlam" instead of glulam, suspended flooring, indoor furniture, wood handicrafts, and even snowboards, using wood welding technology (Bocquet *et al.* 2007; Omrani *et al.* 2007; Belleville *et al.* 2011; O'Loinsigh *et al.* 2012; Segovia *et al.* 2013; Zhang *et al.* 2017). Finally, improvement of the water resistance of welded wood joints from linear-vibration and rotational welding processes has also been studied. Optimization of the welding parameters, the pre- or post-modification of the samples, and impregnation of the water-proofing agents have all been the main kinds of approaches taken by other research groups (Mansouri *et al.* 2009; Pizzi *et al.* 2011, 2013). Although the usefulness of these methods is great, there is still potential for improvement.

End-grain-to-end-grain welding has been attempted before, but in previous studies it did not appear to yield satisfactory results in many wood species of low density, such as spruce. The first successful cases were reported with three high-density Australian eucalyptus woods (with densities around 800 kg/m^3 to 900 kg/m^3) and for beech and oak; all had moderate weld strength (Mansouri *et al.* 2010). If end-grain butt joints obtained by welding can be successfully developed, then they can be used to substitute for finger joints, which have been widely used to join two long pieces of timber end-to-end. Moreover, any technical situation that requires the expansion of the length of a piece of wood can be resolved *via* end-grain-to-end-grain welding technology. This would result in time-savings and lower costs. Also, an eco-friendly process, such as linear vibration welding, would be able to play a prominent role in the wood industry.

The gluing demand of bamboo is as big as the gluing demand of wood. In China, bamboo is the second most-used industrial biomass material after wood. Bamboo requires bonding to produce common construction materials, such as beams, columns, panels, decorative things, and especially bamboo articles, for daily use (Li *et al.* 2016a,b). The special structure of bamboo, which is regarded as a natural fiber (it contains vascular bundles), also contributes to the development of reinforced composites, and it may have some interesting properties when welded. It is not known, for instance, how the ground parenchyma and vascular bundles contribute to the welding interface. Research can also make contributions to the welding technology used in the composite materials. The focus of this article is the development of moso bamboo end-grain butt joints obtained by linear friction welding. The objectives of this work were as follows: (1) to determine whether moso bamboo was suitable to bond with welding technology in the end-grain direction, and (2) to find any special characteristics in welded end-grain butt bamboo joints.

EXPERIMENTAL

Materials

Four-year-old moso bamboo (*Phyllostachys pubescens*) was collected from a bamboo plantation located in the Anhui Province of China. The average density of the collected bamboo was 0.68 g/cm^3 with variation of 1.02 g/cm^3 ± 0.6 g/cm^3 near the outer surface and 0.57 g/cm^3 ± 0.5 g/cm^3 near the inner surface. The moso bamboo was first cut into slats; these slats were then planed and glued together with an isocyanate adhesive to form the panels with 20 mm thickness, 200 mm width, and 1000 mm length. For the linear

vibration welding, the well-prepared bamboo panels were cut perpendicular to the bamboo fiber such that the samples would have dimensions of 20 mm × 20 mm × 200 mm; two of the panels were then end-grain-to-end-grain welded together to form a joint with dimensions of 40 mm × 20 mm × 200 mm.

Linear vibration welding

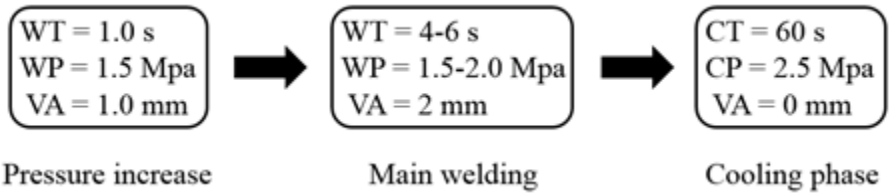

Fig. 1. The welding process

The KLN Ultraschall LVW-2261 machine (Mecasonic, Crest group, Annemasse, France), which was formerly designed for welding thermoplastics, was used here with complete process control. Its vibration welding frequency was 150 Hz. The whole welding process can be divided into two stages: the main welding phase and the cooling pressure-holding phase. In the cooling pressure-holding phase, there was no friction applied to the samples and the amplitude was zero. The cooling phase lasted for 60 s and occurred at a pressure of 2.5 MPa. To ensure that the temperature rose smoothly in the welded surfaces, the main welding process was split into two phases. The first phase was the pressure increasing phase; this involved a 1 s welding time, a 1.5 MPa welding pressure, and a 1 mm vibration amplitude. The second phase mainly contributed to the final tensile-shear strength of the welded joints. Table 1 shows the different parameters to which the machine was programmed. The welding pressure was varied between 1.5 MPa and 2.5 MPa in 0.25 MPa increments, and it was changed to find the final best strength. The amplitude was 2 mm and the welding time was 5 s to 7 s (Fig. 1). The total welding time including the welding pressure rising time was 6 s to 8 s. The moisture content of the moso bamboo samples before welding was 12%; this moisture content (MC) was constant due to the speed of the welding process.

Methods

Temperature measurement at the welding interface

The temperature at the welding interface during the linear vibration welding was measured to record and control the process. The measurement system was made up of a thermo-element with measurement accuracy 0.5%, type K thermocouples (Ni-Cr-Ni alloy, measurement range: -180 °C to 1200 °C), a multi-channel temperature data logging device JK-40U, and the supporting software JK-XU (Jinko, 1.0, Changzhou, China) for the device. Five thermocouples per welded specimen were used. They were positioned in the center of the weld, as well as 5 cm and 1 cm from the edges. The thermocouples were inserted into holes 0.5 mm in diameter with the middle thickness in contact with the welding interface from the side of the welded samples, and the data were conducted using statistical software data processing SPSS 17.0 (Armonk, NY).

Bonding strength measurement

The bonding strength of welded joints were tested using the compression shear test. The test specimen and the procedure were in agreement with GB/T 17517 (1998). The

width of the specimen was 1 cm. The length of the longer part of samples was 4 cm and with 2 cm in the short part. The loading was applied on the longer part of the samples. The loading speed used was 2 mm/min. The time for the failure to research was kept between 30 s and 90 s. The Instron universal testing machine (INSTRON 5848 Microtester, Norwood, USA) used here can record the force and displacement during the test. The compression shear strength was obtained by dividing the maximum force by the bonding area. All samples were stored for 7 days at 20 °C and 65% relative humidity to ensure they has a constant moisture content. Every group had twenty replicates. The SPSS 17.0 statistical software package was used for data processing and analysis.

Density profile measurement and microstructure observation

The welded joints were also observed directly using a Hitachi Tabletop Microscope SEM TM 3000 (Hitachi High-Technologies Corporation, Tokyo, Japan) at an accelerating voltage of 15 kV.

The vertical density profiles of the welded joints were measured using an X-ray densitometer (GreCon DAX-5000, GreCon, Alfeld, Germany). Every 0.02 mm along the thickness of the samples was tested using X-ray attenuation with an accuracy of ± 1%. The scan started from one of the surfaces of the welded samples and proceeded to the other surface, so that the welded layer was in the center of the density profiles.

Energy release rate measurement

There are different methods for the determination of the energy release rate G_{IC}. These methods can be either experimental or analytical. The evaluation of the energy release rates of the linear friction welded butt joints of moso bamboo was performed using the method of experimental compliance with double cantilever beam (DCB) specimens. Because it is more accurate to describe the real behavior of a DCB-type specimen for the case of the wood/adhesive couple, the final dimensions of the test specimens are illustrated in Fig. 2.

Fig. 2. DCB specimen of moso bamboo

A uniaxial testing machine (INSTRON 5848 Microtester, Norwood, USA) with a 2 kN load cell and constant pulling rate of 2 mm per min was used to perform the DCB test. Two metal loading blocks, which were used to apply a load while maintaining a hole in the center of the setup for temperature measurement, were glued onto the two open surfaces of the specimen. All of the loading processes were recorded using an HD camera (Cannon C500 PL, Tokyo, Japan) to measure the crack length on each specimen with a precision of 0.5 mm. The load, displacement, and photographs of the crack tips were

recorded and stored for evaluation. The change of MC of the specimens during the testing was minimal, and its effects were negligible.

RESULTS AND DISCUSSION

The temperature in the welding interface of the butt joints of the moso bamboo specimens as a function of welding time is shown in Fig. 3. The temperature in the welded interface along the welding direction had no significant differences across the samples using a one-way ANOVA test, so the temperature at each time was calculated using an average of the five values.

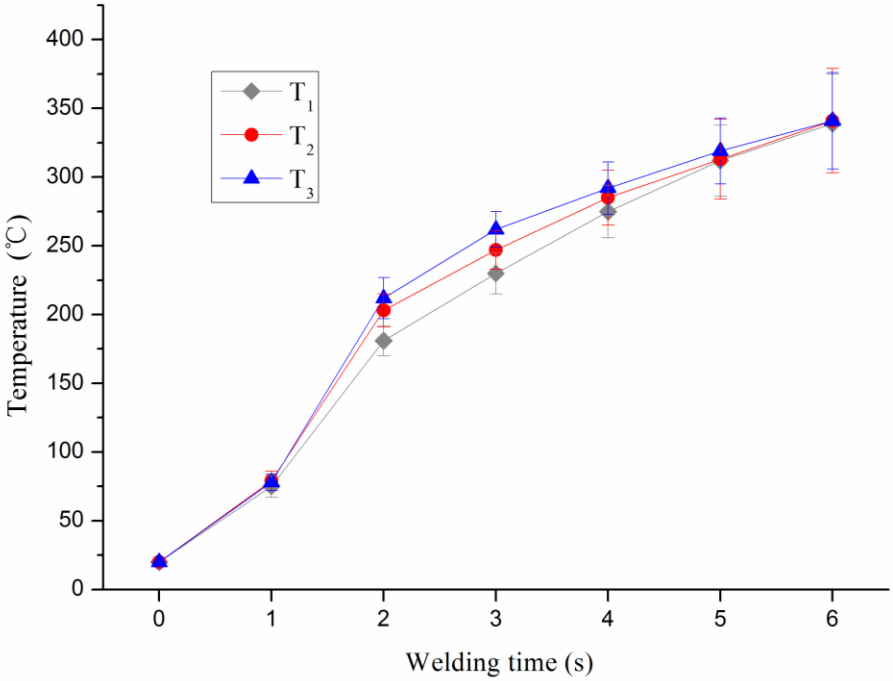

Fig. 3. Temperature of the welded interface at progressive welding times (T means the interface temperature and the subscript 1, 2, and 3 correspond to the sample No. in table 1)

The first three groups (Table 1) had an increased welding pressure that was recorded. Accounting for the different welding pressures, the fastest increase in temperature was seen in the highest welding pressure, 2 MPa, at the beginning of the 4 s welding. Although after that, the differences between the three conditions were not obvious. The welding interface reached approximately 350 °C in approximately 6 s. After this point the temperature increase of the welding interface was very limited. During the holding-cooling step, the temperature decreased to 100 °C after 40 s to 50 s. This supported the choice to set the holding and cooling time to 60 s. During the welding-heating mode, the temperature firstly increased almost straight in the first 1 s. After 1 s to 2 s the standard deviation of the interface temperature became higher. As has been shown by many researchers before, the path of the temperature rise depended on the structure and density of the welded material and the improvement of the standard deviation later was due to the disturbance of the water and compositions in the welded interface (Ganne-Chédeville e*t al.* 2006b).

The average compression shear strength of the end-grain butt joints obtained by friction welding of moso bamboo prepared under different conditions is shown in Table 1. The welding pressure for the first three groups rose with 0.25 MPa of applied pressure to reflect the influence of the pressure. The welding time was also studied within a range of 4 s to 6 s in the main welding procedure. Based on the parameters in Table 1, to obtain the best strength of the end-grain butt joints, the welding pressure must be increased and the welding time must also be prolonged (within limit) compared to the parameters used for welding bamboo longitudinally along its fibers. The welding parameters chosen determined the energy used to produce the welded joints. In other words, in the case of little difference in the coefficient of friction between samples, higher welding pressure and a longer welding time meant that during welding there was more mechanical energy converted into heat to obtain the final welded joints. The energy consumed to obtain the final welded end-grain butt joints of the first three groups was approximately 3.0 kJ ± 0.3 kJ, 3.2 kJ ± 0.3 kJ, and 3.5 kJ ± 0.3 kJ, respectively. Longitudinal welding along the bamboo fiber consumed approximately 2.4 kJ ± 0.3 kJ for the best welding strength. Therefore, the end-grain butt joints of welded bamboo consumed more energy to produce a welded interface due to the hard, vascular bundles present in the bamboo.

Table 1. Compression Strength of End-grain Butt Joints Obtained by Friction Welding of Moso Bamboo

Sample No.	Parameters of Welding Cycle			Compression Strength	
	Time (s)	Pressure (MPa)	Amplitude (mm)	Mean (MPa))	SD (MPa)
1	1/5/60	1.5/1.5/2.5	1/2/0	5.01	0.89
2	1/5/60	1.5/1.75/2.5	1/2/0	5.63	0.77
3	1/5/60	1.5/2/2.5	1/2/0	5.81	0.69
4	1/4/60	1.5/2/2.5	1/2/0	5.05	0.84
5	1/6/60	1.5/2/2.5	1/2/0	5.35	0.77

The results in Table 1 indicated that the average strengths of the groups were all higher than 5 MPa and that the strongest one had a compression strength of 5.81 MPa. There was no significant difference between 1.75 MPa and 2 MPa when the results were analyzed *via* a t-test. It was seen that applying 1.5 MPa significantly reduced the welded bonding strength of a sample, compared to the other pressures. The difference between the groups with 4 s, 5 s, and 6 s welding time was also statistically significant with a p-value of 0.023. The optimized conditions used to create the strongest end-grain butt joints of the welded moso bamboo were 1.75 MPa to 2.0 MPa and 5 s welding time with a 2-mm vibration amplitude.

Although the welded strength of the produced end-grain butt joints was lower than for longitudinally-welded bamboo (Zhang *et al.* 2014a) and the standard deviation between samples was higher, it was not easy to successfully create end-grain-to-end-grain welded joints. This was due to the friction force present during the welding process, the interface wood fibers being cleaved in the vibration direction, and the friction force decrease, hence it eliminated the possibility of welding as stated in the introduction. Thus, it was interesting to obtain high weld strength in the end-grain butt joints of moso bamboo. Because splits could easily happen in bamboo, the average density of the moso bamboo was approximately 650 kg/m^3 ± 50 kg/m^3, and the density of the inner part of the bamboo was even lower due to the vascular bundles distributed in the transverse section of the bamboo.

This may have been due to the specific structure of the bamboo. The microstructure of the welded layer observed *via* SEM could help to explain these results.

As it is known, in longitudinal welding along the wood fibers, a composite of wood fibers entangled in the matrix of molten intercellular materials is formed at the welded interface, yielding the final welded joint. However, the relative position of the fibers is totally different between the end-grain-to-end-grain welding and in longitudinal fiber welding. The same kind of welded-interphase morphology cannot occur in the end-grain butt joints obtained by welding. Figure 4 shows the full view of the welded end-grain butt joints. The bamboo is mainly composed of vascular bundles and parenchymal cells. The vascular bundles, which are very hard, are the reinforcing phases, while the parenchymal cells are very soft, and thus they serve as the matrix of this natural composite material. The huge differences in the mechanical properties between parenchymal cells and vascular bundles cause the rather different morphology of the welded layer. The parenchymal cells are broken and melted to form the continuous welding layer due to the thermal and mechanical action during welding, while the vascular bundles are not melted by the heat. However, the vascular bundles are bent by the vibrations in mechanical welding. They may bend to one side, are prominent on the welded surface, and insert themselves into the welded molten material. The authors did not find entangled bamboo fibers in the welded layer, which was quite common in the welded joints along the bamboo fiber; the bent vascular bundles might have mainly contributed to the strength of the welded joints, though. The microstructure of the welded end-grain butt joints had some similarities with the "finger-joint" appearance.

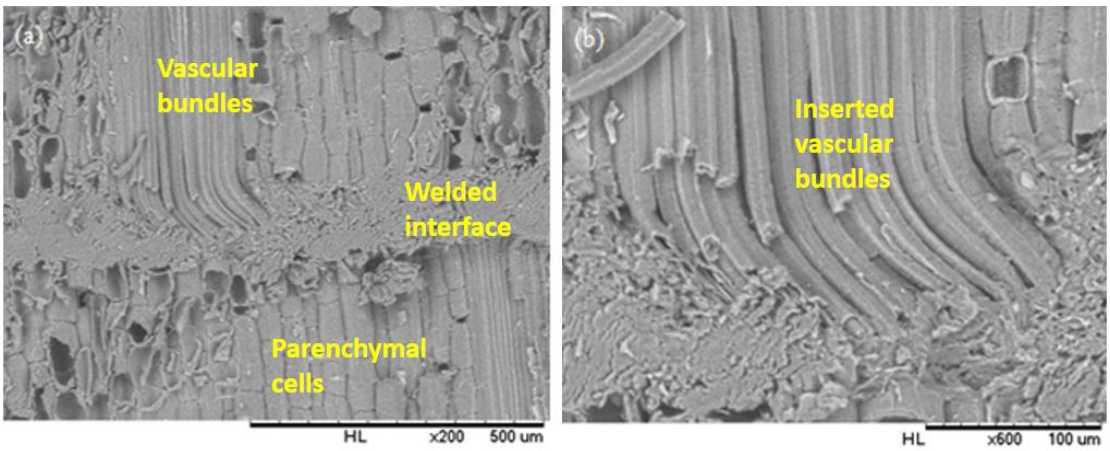

Fig. 4. Welded end-grain butt joints of moso bamboo showing the entire welded interface (a) and the bent vascular bundles resulting from the welding process (b)

In the entire welded interface, the authors did not find large cracks along the bamboo fiber in the welded surfaces, which could be observed in the end-grain-to-end-grain welded surface of beech wood. During end-grain bamboo welding, the parenchymal cells were broken and melted first, which made the vascular bundles become prominent in the welded interface. The vascular bundles were then the main constituent affected by welding pressure and friction force. Under these conditions, the bent vascular bundles protected the parenchymal cells on the surface of the weld from cracking. This weld can be thought of as similar to the welding of two brushes.

The section of the weld that withstands the lateral friction produced from the linear vibration welding is mainly the protrusive vascular bundles in the welded surface of the moso bamboo. This is the reason why defibration does not happen in the end-grain-to-end-grain welding process of the moso bamboo, notwithstanding the material having a low density. This is the natural structure of moso bamboo that differentiates it from wood and allows for the possibility to obtain welded end-grain butt joints of good strength. Due to the effect of the vascular bundles in the welded surface, the maximum density of the welded joints was not as high as in the welding along the bamboo fiber. Figure 5 shows the welded joints reached a maximum density that was different along the bamboo fiber welded joints.

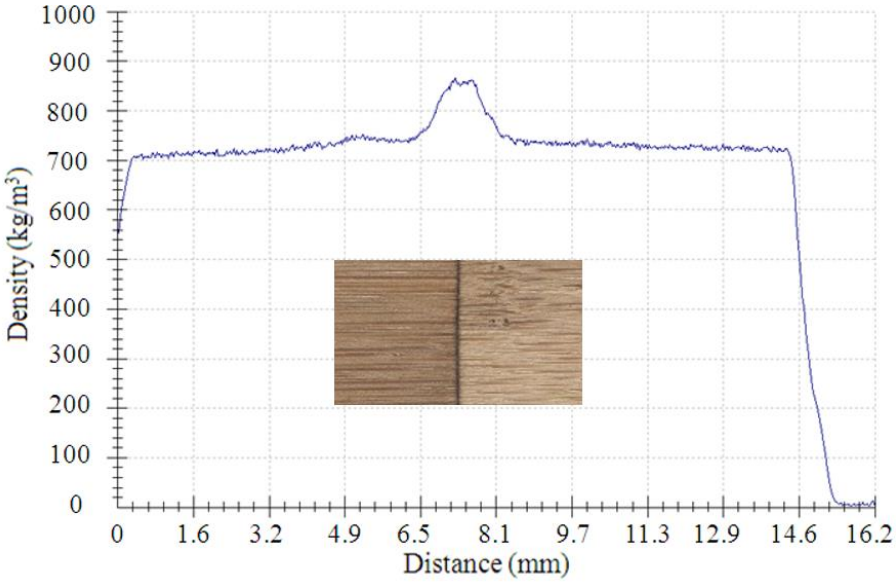

Fig. 5. Density profile of the end-grain butt joints from friction-welded moso bamboo

The energy release rates of the wood bonding environments are mainly influenced by the rigidity and strength of the adhesive, the interfaces, or both. Wang *et al.* (2014) performed mechanical tests on natural bamboo, as well as on the adhesive. The energy release rate of the DCB test of the bamboo perpendicular to the fiber were in the range of 400 J/m^2 to 1500 J/m^2, and the bamboo knots especially had a great effect on the performance of the overall material. Here, the values obtained for the energy release rate of welded end-to-end butt joints of moso bamboo were much lower than the amount due to the discontinuity of the high strength of the vascular bundles in the bamboo. However, a comparison should be made between the common commercial adhesions used in the bamboo. In the literature, only a few references could be found concerning the calculation of the energy release rate (G_{IC}) for the adhesively-bonded joints with butt joints. However, the measurement of the energy release rate of wood joints bonded with conventional thermosetting adhesives, which range from 100 J/m^2 to 300 J/m^2, can yield some references (Ganne-Chédeville *et al.* 2008). An average value of 161 J/m^2 corresponded to this classical range, and this value could be even greater than the value in some soft wood adhesives (Table 2). Meanwhile, the variation coefficient of the welded moso bamboo joints, which were in the ranges of 20% to 40%, was much lower than the range measured for adhesive joints, which could reach to up to 100%. In the case of wood-adhesive joints, crack propagation occurred randomly in the adhesive, the interface, and in the wood. For the welded butt joints of moso bamboo, the fracture took place almost completely in the

interface. The broken surface of the welded joints did not show any original moso bamboo; therefore, the value of G_{IC} obtained was likely a specific characteristic of the pure joints. The average energy release rate for the welded beech wood was approximately 106 J/m^2, which was approximately 52% smaller than the authors measured in this study, due to the special structure of the micro finger constructed by the interface vascular bundles.

Table 2. Values for Energy Release Rate G_{IC}, Crack Length, and Standard Deviation (SD) for Welded Butt Joints of Moso Bamboo

Parameters	Loading/Unloading Cycle Number						Average G_{IC} (J/m^2)
	1	2	3	4	5	6	
a (m)	0.05	0.08	0.11	0.13	0.15	0.17	-
G_{IC}	185	169	173	154	143	139	161
SD	42	38	41	38	32	30	-

Note: a is the pre-served crack length

CONCLUSIONS

1. End-grain butt joints created with high compression shear strength *via* the linear vibration welding of moso bamboo were obtained.
2. Defibration, which usually occurred with lower-density woods in end-grain welds due to friction, did not happen in welds with moso bamboo. Using moso bamboo guaranteed a satisfactory joint strength that cannot be obtained in most other wood species with lower-to-mid-range densities.
3. The hard, vascular bundles within bamboo that emerge from the weld surface during welding partially endured the friction generated by the linear vibration used to weld, and prevented the end-grain of the bamboo from cracking during the abrasion of the two "brushes" that made up the two separate ends of the bamboo segments. The final morphology of the welded joint was like fingerjoints, with the vascular bundles of the two-opposing surfaces connected with each other by resolidification of the molten parenchymal cells.

ACKNOWLEDGMENTS

The authors are grateful for support from the Science and Technology Department of Jiangsu Province under Grant BK20150878, the Chinese Forestry Administration under Grant 2015-4-57, the Nanjing Forestry University under Grant cx201617, and the Priority Academic Program Development of Jiangsu Higher Education Institutions (PAPD).

REFERENCES CITED

Amirou, S., Pizzi, A., and Luo, H. (2016). "Variation of shear properties of welded spruce at different pressures and welding times," *Biotribology* 5, 61-66. DOI: 10.1016/j.biotri.2015.09.001

Bocquet, J. F., Pizzi, A., and Resch, L. (2007). "Full-scale industrial wood floor assembly and structures by welded-through dowels," *Holz als Roh- und Werkstoff* 65(2), 149-155. DOI: 10.1007/s00107-006-0170-4

Belleville, B., Segovia, C., Pizzi, A., Stevanovic, T., and Cloutier, A. (2011). "Wood blockboards fabricated by rotational dowel welding," *Journal of Adhesion Science and Technology* 25(20), 2745-2753. DOI: 10.1163/016942410X537323

Belleville, B., Stevanovic, T., Cloutier, A., Pizzi, A., Prado, M., Erakovic, S., and Royer, M. (2013). "An investigation of thermochemical changes in Canadian hardwood species during wood welding," *European Journal of Wood and Wood Products* 71(2), 245-257. DOI: 10.1007/s00107-013-0671-x

Delmotte, L., Ganne-Chédeville, C., Leban, J. M., Pizzi, A., and Pichelin, F. (2008). "CP-MAS, ^{13}C NMR and FT-IR investigation of the degradation reactions of polymer constituents in wood welding," *Polymer Degradation and Stability* 93(2), 406-412. DOI: 10.1016/j.polymdegradstab.2007.11.020

GB/T 17517 (1998). "Adhesives – Wood to wood adhesive bonds – Determination of shear strength by compression loading," Standardization Administration of China, Beijing, China.

Ganne-Chédeville, C., Leban, J. M., Properzi, M., Pichelin, F., and Pizzi, A. (2006a). "Temperature and density distribution in mechanical vibration wood welding," *Wood Science and Technology* 40(1), 72-76. DOI: 10.1007/s00226-005-0037-6

Ganne-Chédeville, C., Properzi, M., Pizzi, A., Leban, J. M., and Pichelin, F. (2006b). "Parameters of wood welding: A study with infrared thermography," *Holzforschung* 60(4), 434-438. DOI: 10.1515/HF.2006.068

Ganne-Chédeville, C., Duchanois, G., Pizzi, A., Pichelin, F., Properzi, M., and Leban, J. M. (2008). "Wood welded connections: Energy release rate measurement," *Journal of Adhesion Science and Technology* 22(2), 169-179. DOI: 10.1163/156856108X306939

Gfeller, B., Zanetti, M., Properzi, M., Pizzi, A., Pichelin, F., Lehmann, M., and Delmotte, L. (2003). "Wood bonding by vibrational welding," *Journal of Adhesion Science and Technology* 17(11), 1573-1589. DOI: 10.1163/156856103769207419

Li, Y., Xu, B., Zhang, Q., and Jiang, S. (2016a). "Present situation and the countermeasure analysis of bamboo timber processing industry in China," Journal of Forestry Engineering 1(1), 2-7. DOI: 10.13360/j.issn.2096-1359.2016.01.001

Li, H., Zhang, Q., Wu, G., Xiong, X., and Li, Y. (2016b). "A review on development of laminated bamboo lumber," *Journal of Forestry Engineering* 1(6), 10-16. DOI: 10.13360/j.issn.2096-1359.2016.06.002

Mansouri, H. R., Omrani, P., and Pizzi, A. (2009). "Improving the water resistance of linear vibration-welded wood joints," *Journal of Adhesion Science and Technology* 23(1), 63-70. DOI: 10.1163/156856108X335595

Mansouri, H. R., Pizzi, A., and Leban, J. M. (2010). "End-grain butt joints obtained by friction welding of high density eucalyptus wood," *Wood Science and Technology* 44(3), 399-406. DOI: 10.1007/s00226-010-0349-z

Omrani, P., Bocquet, J. F., Pizzi, A., Leban, J. M., and Mansouri, H. (2007). "Zig-zag rotational dowel welding for exterior wood joints," *Journal of Adhesion Science and Technology* 21(10), 923-933. DOI: 10.1163/156856107781393910

Omrani, P., Mansouri, H. R., and Pizzi, A. (2009). "Linear welding of grooved wood surfaces," *European Journal of Wood and Wood Products* 67, 479-481. DOI: 10.1007/s00107-009-0334-0

O'Loinsigh, C., Oudjene, M., Shotton, E., Pizzi, A., and Fanning, P. (2012). "Mechanical behaviour and 3D stress analysis of multi-layered wooden beams made with welded-through wood dowels," *Composite Structures* 94(2), 313-321. DOI: 10.1016/j.compstruct.2011.08.029

Pizzi, A., Leban, J. M., Kanazawa, F., Properzi, M., and Pichelin, F. (2004). "Wood dowel bonding by high-speed rotation welding," *Journal of Adhesion Science and Technology* 18(11), 1263-1278. DOI: 10.1163/1568561041588192

Pizzi, A., Mansouri, H. R., Leban, J. M., Delmotte, L., and Pichelin, F. (2011). "Enhancing the exterior performance of wood joined by linear and rotational welding," *Journal of Adhesion Science and Technology* 25(19), 2717-2730. DOI: 10.1163/016942411X556088

Pizzi, A., Zhou, X., Navarrete, P., Segovia, C., Mansouri, H. R., Placentia Pena, M. I., and Pichelin, F. (2013). "Enhancing water resistance of welded dowel wood joints by acetylated lignin," *Journal of Adhesion Science and Technology* 27(3), 252-262. DOI: 10.1080/01694243.2012.705512

Properzi, M., Leban, J. M., Pizzi, A., Wieland, S., Pichelin, F., and Lehmann, M. (2005). "Influence of grain direction in vibrational wood welding," *Holzforschung* 59(1), 23-27. DOI: 10.1515/HF.2005.004

Ruponen, J., Čermák, P., Rhême, M., Miettinen, A., Rohumaa, A., and Rautkari, L. (2015). "Influence of welding time on tensile-shear strength of linear friction welded birch (*Betula pendula* L.) wood," *BioResources* 10(2), 3481-3491.

Segovia, C., Zhou, X., and Pizzi, A. (2013). "Wood blockboards for construction fabricated by wood welding with pre-oiled dowels," *Journal of Adhesion Science and Technology* 27(5-6), 577-585. DOI: 10.1080/01694243.2012.690616

Stamm, B., Natterer, J., and Navi, P. (2005). "Joining wood by friction welding," *Holz als Roh- und Werkstoff* 63(5), 313-320. DOI: 10.1007/s00107-005-0007-6

Tondi, G., Andrews, S., Pizzi, A., and Leban, J. M. (2007). "Comparative potential of alternative wood welding systems, ultrasonic and microfriction stir welding," *Journal of Adhesion Science and Technology* 21(16), 1633-1643. DOI: 10.1163/156856107782793258

Wang, F., Shao, Z., Wu, Y., and Wu, D. (2014). "The toughness contribution of bamboo node to the Mode I interlaminar fracture toughness of bamboo," *Wood Science and Technology* 48(6), 1257-1268. DOI: 10.1007/s00226-013-0591-2

Zhang, H., Pizzi, A., Lu, X., and Zhou, X. (2014a). "Optimization of tensile shear strength of linear mechanically welded outer-to-inner flattened moso bamboo (*Phyllostachys pubescens*)," *BioResources* 9(2), 2500-2508.

Zhang, H., Pizzi, A., Zhou, X., Lu, X., and Janin, G. (2014b). "Comparison of linear vibration welded joints in three different directions of wood tauari *(Couratari oblongifilia*)," *International Wood Products Journal* 5(4), 228-232. DOI: 10.1179/2042645314Y.0000000081

Zhang, H., Pizzi, A., Zhou, X., Lu, X., and Wang, Z. (2017). "The study of linear vibrational welding of moso bamboo," *Journal of Adhesion Science and Technology* DOI: 10.1080/01694243.2017.1322767

Zigon, J., Pizzi, A., zhang, H., Sega, B., Cop, M., and Sernek, M. (2015). "The influence of heat and chemical treatments of beech wood on the shear strength of welded and UF bonded specimens," *European Journal of Wood and Wood Products* 73(5), 685-687. DOI: 10.1007/s00107-015-0930-0

Article submitted: March 1, 2017; Peer review completed: May 20, 2017; Revised version received: June 17, 2017; Accepted: July 2, 2017; Published: July 19, 2017.
DOI: 10.15376/biores.12.3.6446-6457